

# First Step Toward the Quantitative Identification of Peptide $3_{10}$ -Helix Conformation with NMR Spectroscopy: NMR and X-ray Diffraction Structural Analysis of a Fully-Developed $3_{10}$ -Helical Peptide Standard

Rainer Gratias,<sup>†</sup> Robert Konat,<sup>†</sup> Horst Kessler,<sup>\*,†</sup> Marco Crisma,<sup>‡</sup> Giovanni Valle,<sup>‡</sup> Alessandra Polese,<sup>‡</sup> Fernando Formaggio,<sup>‡</sup> Claudio Toniolo,<sup>\*,‡</sup> Quirinus B. Broxterman,<sup>§</sup> and Johan Kamphuis<sup>#</sup>

Contribution from the Institut für Organische Chemie und Biochemie, Technische Universität München, D-85747 Garching, Germany, Biopolymer Research Center, CNR, Department of Organic Chemistry, University of Padova, 35131 Padova, Italy, DSM Research, Organic Chemistry and Biotechnology Section, P.O. Box 18, 6160 MD Geleen, The Netherlands, and DSM Fine Chemicals, 6401 JH Heerlen, The Netherlands

Received September 8, 1997

**Abstract:** We have synthesized by solution methods and fully characterized the N<sup>α</sup>-blocked heptapeptide methylamide *m*BrBz-[L-Iva-L-(αMe)Val]<sub>2</sub>-L-(αMe)Phe-L-(αMe)Val-L-Iva-NHMe, fully based on conformationally constrained C<sup>α</sup>-methylated α-amino acids. An X-ray diffraction investigation of the N<sup>α</sup>-benzyloxy-carbonylated analogue showed that in the crystal state both independent molecules (**A** and **B**) in the asymmetric unit of the peptide adopt a fully developed, regular, right-handed  $3_{10}$ -helical structure, although molecule **A** would be slightly distorted at the C-terminal residue. Solution conformational analysis on the *m*BrBz-blocked peptide was carried out in CDCl<sub>3</sub> by means of NMR spectroscopy. For structure determination we performed restrained molecular dynamics simulations in CDCl<sub>3</sub> based on a search of the conformational space derived from a simulated annealing strategy. For this peptide the NMR observables can be described by a single backbone conformation, more specifically a rigid  $3_{10}$ -helix spanning the amino acid sequence from residue 1 to residue 6. The C-terminal methylamido NH group seems to be involved simultaneously in two H-bonds (with the preceding *i* - 3 and *i* - 4 carbonyl groups). Although in this peptide model there are no distinct NOE distances for discriminating  $3_{10}$ - versus α-helix conformation, the sum of all NMR-derived restraints clearly results in a  $3_{10}$ -helical structure. Convergence from different starting structures (including an α-helix) into a  $3_{10}$ -helix was observed.

## Introduction

The  $3_{10}$ -helix, first predicted as a reasonably stable polypeptide secondary structure about 55 years ago,<sup>1</sup> has only relatively recently attracted the attention of structural biochemists and protein crystallographers.<sup>2,3</sup> Besides the classical α-helix and β-pleated sheet conformation, it represents the third principal, long-range structural element occurring in globular proteins and has been described at atomic resolution in model peptides and in peptaibol antibiotics.<sup>4</sup> The average conformational parameters of the α-helix are close to those of the  $3_{10}$ -helix, the latter being slightly tighter and more elongated.<sup>4</sup> In particular, the backbone φ,ψ torsion angles for the two helices differ only by 6° and 12°, respectively. However, the C=O...H-N intramolecular H-bonding schemes are different, *i* ← *i* + 3 for the  $3_{10}$ -helix, while *i* ← *i* + 4 for the α-helix.

Nuclear magnetic resonance (NMR) is the most extensively used spectroscopic technique to determine secondary structural

information at the residue level in peptides and proteins in solution.<sup>5–7</sup> NMR is expected to give parameters that are unique for each of the two helix types.<sup>7,8</sup> An overwhelming amount of information is available on the various interproton through-space connectivities and the relative intensities of the resulting NOE peaks for peptide and protein α-helices. Despite some promising, initial attempts,<sup>9,10</sup> a similar analysis of  $3_{10}$ -helices has not been carried out in detail yet. In part, this may be ascribed to the difficulty of finding a peptide model that could adopt *exclusively* the  $3_{10}$ -helical conformation in solution and could be suitable for NMR analysis in terms of amino acid sequence. In addition, there are only a few short-range distances which can be used to distinguish the two helical types. Only *d*<sub>αN</sub>(*i*, *i* + 2) differs by 0.6 Å (4.4 Å for the α-helix, and 3.8 Å for the  $3_{10}$ -helix), but distances above 4 Å already give rise to very weak signal intensities.

(5) Kessler, H.; Seip, S. In *Two-Dimensional NMR Spectroscopy*; Goasmun, W. R., Carlson, R. M. K., Eds.; VCH: Weinheim, 1994; pp 619–654.

(6) Kessler, H.; Schmitt, W. In *Encyclopedia of NMR*; Grant, D. M., Harris, R. K., Eds.; Wiley: Chichester, 1996; Vol. 6, pp 3527–3537.

(7) Wüthrich, K. *NMR of Proteins and Nucleic Acids*; Wiley: New York, 1986.

(8) Wüthrich, K.; Billeter, M.; Braun, W. *J. Mol. Biol.* **1984**, *180*, 715–740.

(9) Basu, G.; Kuki, A. *Biopolymers* **1993**, *33*, 995–1000.

(10) Millhauser, G. L.; Stenland, C. J.; Hanson, P.; Bolin, K. A.; van de Ven, F. J. M. *J. Mol. Biol.* **1997**, *267*, 963–974.

<sup>†</sup> Technische Universität München.

<sup>‡</sup> University of Padova.

<sup>§</sup> DSM Research.

<sup>#</sup> DSM Fine Chemicals.

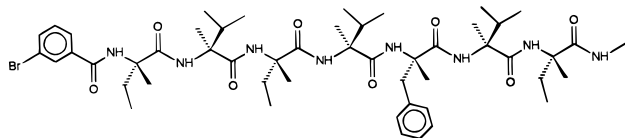
(1) Taylor, H. S. *Proc. Am. Phyl. Soc.* **1941**, *85*, 1–7.

(2) Barlow, D. J.; Thornton, J. M. *J. Mol. Biol.* **1988**, *201*, 601–619.

(3) Peters, J. W.; Stowell, H. B.; Rees, D. C. *Nature: Struct. Biol.* **1996**, *3*, 991–994.

(4) Toniolo, C.; Benedetti, E. *Trends Biochem. Sci.* **1991**, *16*, 350–353.

Works from our as well as other laboratories have firmly established that most of the  $C^\alpha$ -tetrasubstituted  $\alpha$ -amino acids are strong promoters of  $3_{10}$ / $\alpha$ -helical conformations.<sup>11–13</sup> In particular, heteropeptides containing only  $C^\alpha$ -methylated amino acid residues and homopeptides from  $C^\alpha$ -methylated amino acids, such as Aib ( $\alpha$ -aminoisobutyric acid or  $C^\alpha$ -methylalanine), Iva (isovaline or  $C^\alpha$ -methyl- $\alpha$ -aminobutyric acid), ( $\alpha$ Me)Val ( $C^\alpha$ -methylvaline), and ( $\alpha$ Me)Phe ( $C^\alpha$ -methylphenylalanine), adopt *exclusively* the  $3_{10}$ -helical conformation in the crystal state and in solvents of low polarity. Fully developed, stable  $3_{10}$ -helices were observed in these solvents at the level of  $N^\alpha$ -blocked heptapeptide amides or octapeptide esters. Therefore, the most reliable standard peptide model for the first unambiguous structural determination of a completely assigned  $3_{10}$ -helical conformation by NMR must be constructed with  $C^\alpha$ -methylated amino acid residues. With this information in mind, as a model peptide for the NMR characterization of the  $3_{10}$ -helical conformation, we decided to synthesize the  $N^\alpha$ -blocked heptapeptide methylamide *m*BrBz-[L-Iva-L-( $\alpha$ Me)Val]<sub>2</sub>-L-( $\alpha$ Me)Phe-L-( $\alpha$ Me)-Val-L-Iva-NHMe (*m*BrBz, *m*-bromobenzoyl; NHMe, methyl-amino).



Such a sequence was designed with the aim of minimizing the ambiguities in the assignment of the NMR resonances. We have judged it worthwhile to obtain also the X-ray diffraction structure of the same peptide sequence as a reference and precise control of the interatomic distances which can be inferred from the NMR analysis.

## Materials and Methods

**Synthesis and Characterization of Peptides.** Melting points were determined with a Leitz (Wetzlar, Germany) model Laborlux 12 apparatus and are not corrected. Optical rotations were measured with a Perkin-Elmer (Norwalk, CT) model 241 polarimeter equipped with a Haake (Karlsruhe, Germany) model D thermostat. Thin-layer chromatography was performed on Merck (Darmstadt, Germany) Kieselgel 60F<sub>254</sub> precoated plates with use of the following solvent systems: 1 (chloroform–ethanol, 9:1); 2 (1-butanol–acetic acid–water, 3:1:1); 3 (toluene – ethanol, 7:1). The chromatograms were examined using ultraviolet fluorescence or developed by chlorine–starch–potassium iodide or ninhydrin chromatic reaction as appropriate. All the compounds were obtained in a chromatographically homogeneous state.

The free  $C^\alpha$ -tetrasubstituted  $\alpha$ -amino acids were  $N^\alpha$ -protected with the benzyloxycarbonyl (Z) group.<sup>14–17</sup> The Z-protected amino acids were activated by using the acid fluoride method.<sup>18</sup> The synthesis and

(11) Karle, I. L.; Balam, P. *Biochemistry* **1990**, *29*, 6747–6756.

(12) Toniolo, C.; Benedetti, E. *Macromolecules* **1991**, *24*, 4004–4009.

(13) Toniolo, C.; Crisma, M.; Formaggio, F.; Valle, G.; Cavicchioli, G.; Précigoux, G.; Aubry, A.; Kamphuis, J. *Biopolymers* **1993**, *33*, 1061–1072.

(14) Formaggio, F.; Crisma, M.; Bonora, G. M.; Pantano, M.; Valle, G.; Toniolo, C.; Aubry, A.; Bayeul, D.; Kamphuis, J. *Pept. Res.* **1995**, *8*, 6–15.

(15) Polese, A.; Formaggio, F.; Crisma, M.; Valle, G.; Toniolo, C.; Bonora, G. M.; Broxterman, Q. B.; Kamphuis, J. *Chem. Eur. J.* **1996**, *2*, 1104–1111.

(16) Toniolo, C.; Crisma, M.; Bonora, G. M.; Klajc, B.; Lelj, F.; Grimaldi, P.; Rosa, A.; Polinelli, S.; Boesten, W. H. J.; Meier, E. M.; Schoemaker, H. E.; Kamphuis, J. *Int. J. Pept. Protein Res.* **1991**, *38*, 242–252.

(17) Toniolo, C.; Formaggio, F.; Crisma, M.; Bonora, G. M.; Pegoraro, S.; Polinelli, S.; Boesten, W. H. J.; Schoemaker, H. E.; Broxterman, Q. B.; Kamphuis, J. *Pept. Res.* **1992**, *5*, 56–61.

**Table I.** Analytical and Physical Properties of the Newly Synthesized Derivatives and Peptides

compd	melting point (°C)	recryst solvent <sup>c</sup>	[ $\alpha$ ] <sub>D</sub> <sup>20</sup> (deg) <sup>b</sup>	TLC			IR (cm <sup>-1</sup> ) <sup>e</sup>
				R <sub>F1</sub>	R <sub>F2</sub>	R <sub>F3</sub>	
Z-L-( $\alpha$ Me)Phe-F	oil		-41.2 <sup>d</sup>				3410, 3339, 1831, 1715, 1521
Z-L-Iva-F	oil		-0.1 <sup>d</sup>				3413, 3343, 1838, 1717, 1615, 1586, 1523
Z-L-Iva-NHMe	oil	AcOEt/PE	-2.2 <sup>f</sup>	0.75	0.90	0.45	3368, 1717, 1652, 1526
Z-L-( $\alpha$ Me)Val-L-Iva-NHMe	109–111	AcOEt/PE	31.6	0.80	0.95	0.40	3372, 3317, 1704, 1655, 1545
Z-L-( $\alpha$ Me)Phe-L-( $\alpha$ Me)Val-L-Iva-NHMe	178–180	AcOEt/PE	7.8	0.80	0.95	0.40	3429, 3338, 1706, 1675, 1646, 1521
Z-L-( $\alpha$ Me)Val-L-( $\alpha$ Me)Phe-L-( $\alpha$ Me)Val-L-Iva-NHMe	193–195	AcOEt/PE	-3.8	0.80	0.95	0.35	3415, 3334, 1702, 1665, 1643, 1528
Z-L-Iva-L-( $\alpha$ Me)Val-L-( $\alpha$ Me)Phe-L-( $\alpha$ Me)Val-L-Iva-NHMe	228–230	AcOEt	35.6	0.75	0.95	0.35	3322, 1699, 1657, 1643, 1525
Z-L-( $\alpha$ Me)Val-L-Iva-L-( $\alpha$ Me)Val-L-Iva-NHMe	231–232	MC/PE	25.2	0.70	0.95	0.35	3323, 1702, 1657, 1526
Z-L-Iva-L-( $\alpha$ Me)Val-L-Iva-L-( $\alpha$ Me)Phe-L-( $\alpha$ Me)Val-L-Iva-NHMe	238–241	AcOEt/Et <sub>2</sub> O/PE	31.4	0.65	0.95	0.30	3323, 1700, 1658, 1526
<i>m</i> BrBz-L-Iva-L-( $\alpha$ Me)Val-L-Iva-L-( $\alpha$ Me)Val-L-Iva-NHMe	302–303	MC/PE	38.3	0.60	0.95	0.40	3310, 1656, 1530

<sup>a</sup> AcOEt, ethyl acetate; PE, petroleum ether; Et<sub>2</sub>O, diethyl ether; MC, methylene chloride. <sup>b</sup>  $c = 0.5$ , methanol. <sup>c</sup> The solid-state IR absorption spectra were obtained in KBr pellets (only bands in the 3450–3300 and 1850–1500 cm<sup>-1</sup> regions are reported). <sup>d</sup>  $c = 0.5$ , methylene chloride. <sup>e</sup> R<sub>F4</sub> (AcOEt-PE, 1:3). <sup>f</sup> [ $\alpha$ ]<sub>365</sub><sup>20</sup>.

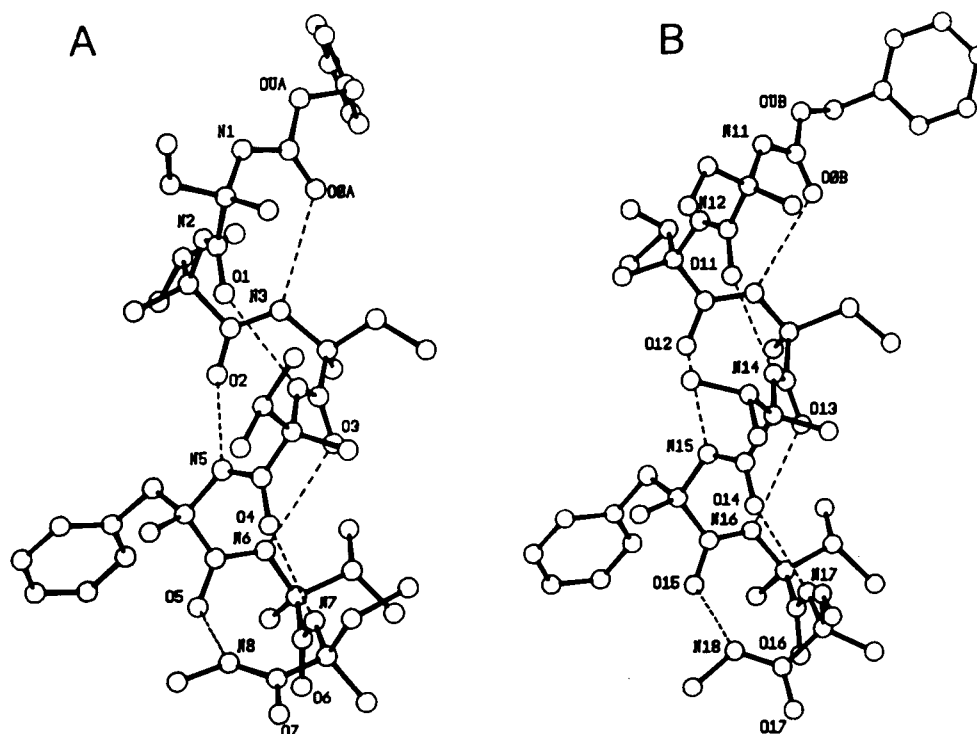


**Figure 1.** X-ray diffraction structure of the two independent molecules (A and B) in the asymmetric unit of Z-[L-Iva-L-( $\alpha$ Me)Val]<sub>2</sub>-L-( $\alpha$ Me)-Phe-L-( $\alpha$ Me)Val-L-Iva-NHMe with atom numbering, as viewed perpendicularly to the helix axis. The intramolecular H-bonds are indicated by dashed lines. As for molecule B, only the conformation with the higher occupancy factor for the ( $\alpha$ Me)Val<sup>12</sup> and Iva<sup>17</sup> side-chain C $\alpha$ -atoms is shown.

**Table 2.** Crystal Data for the Terminally Blocked Heptapeptide

empirical formula	C <sub>52</sub> H <sub>84</sub> N <sub>8</sub> O <sub>9</sub>
mol wt	963.3
temp (K)	293(2)
crystal system	monoclinic
space group	P2 <sub>1</sub>
<i>a</i> (Å)	9.861(2)
<i>b</i> (Å)	18.338(3)
<i>c</i> (Å)	32.023(8)
$\alpha$ (deg)	90
$\beta$ (deg)	98.6(1)
$\gamma$ (deg)	90
vol (Å <sup>3</sup> )	5726(2)
<i>Z</i>	4
molecules/asymmetric unit	2
density (g/cm <sup>3</sup> ) (calcd)	1.117
abs coeff (mm <sup>-1</sup> )	0.618
<i>F</i> (000)	2088
no. of collected reflcns	11459
no. of independent reflcns	8652
<i>R</i> <sub>int</sub>	0.058
no. of data/restraints/parameters	8652/22/1186
goodness of fit	1.033
max shift/esd's	0.118
max and min $\Delta\rho$ (e/Å <sup>3</sup> )	+0.50/−0.21

characterization of Z-L-( $\alpha$ Me)Val-F were already reported,<sup>15</sup> while Z-L-Iva-F and Z-L-( $\alpha$ Me)Phe-F are described here. The Z-group was removed by catalytic hydrogenation. The *m*BrBz moiety was incorporated in the N<sup>α</sup>-deblocked heptapeptide by using *m*BrBz-OAt (OAt, 1-oxy-7-azabenzotriazole).<sup>19</sup> The latter was prepared from the commercially available *m*BrBz-Cl (Fluka, Buchs, Switzerland) and HOAt (Millipore, Bedford, MA) in methylene chloride in the presence of *N*-methylmorpholine [mp 159–160 °C (from ethyl acetate); *R*<sub>F1</sub> 0.95; *R*<sub>F2</sub> 0.95; *R*<sub>F3</sub> 0.75; IR (KBr) 1791, 1591, 1566 cm<sup>-1</sup>. The analytical and physical properties of the newly synthesized peptides are listed in

(18) Carpino, L. A.; Mansour, E. S. M. E.; Sadat-Aalae, D. *J. Org. Chem.* **1991**, *56*, 2611–2614.

(19) Carpino, L. A. *J. Am. Chem. Soc.* **1993**, *115*, 4397–4398.

Table 1. All of the synthetic intermediates were also characterized by <sup>1</sup>H NMR. The final *m*BrBz-protected heptapeptide methylamide was also characterized by (i) amino acid analysis (C.Erba model 3A30 amino acid analyzer, Rodano, Milan, Italy) [Iva 2.9, ( $\alpha$ Me)Val 3.2, ( $\alpha$ Me)-Phe 1.1] and (ii) mass spectrometry (FAB-MS) (MW 1012.1) [1013 (M + H)<sup>+</sup>, 1035 (M + Na)<sup>+</sup>].

**X-ray Diffraction.** Colorless crystals of the terminally blocked heptapeptide were grown from ethanol by slow evaporation. A single crystal of approximate dimensions 0.4 × 0.4 × 0.2 mm was mounted on the tip of a glass capillary. Cell parameters were determined from 25 well-centered reflections in the 15–25°  $\theta$  range. Data collection was performed by using a Philips PW1100 four-circle diffractometer and graphite monochromated Cu K radiation ( $\lambda$  = 1.54184 Å),  $\theta$ –2 $\theta$  scan mode up to 2 $\theta$  = 120.4°, *h* from –11 to 10, *k* from 0 to 20, *l* from 0 to 34.

The structure was solved by direct methods (SHELXS 86 program).<sup>20</sup> Refinement was carried out on *F*<sup>2</sup>, using the full dataset and the SHELXL 93<sup>21</sup> program. For the side chain of ( $\alpha$ Me)Val(12) two positions were assigned to the CG2 atom, with occupancy parameters of 0.55 and 0.45, respectively. Similarly, the CG atom of Iva(17) was refined over two positions with occupancy parameters of 0.60 and 0.40, respectively. These atoms were treated isotropically throughout the refinement. H atoms were included at calculated positions with idealized geometry, and they were allowed to ride on their carrying atom, with *U*<sub>iso</sub> set equal to 1.2 (or 1.5 for methyl groups) times the *U*<sub>eq</sub> of the carrying atom. Restraints were applied to the 1–2 and 1–3 distances involving the side-chain atoms of the ( $\alpha$ Me)Val(12) residue, the CB1 atom of Iva(13), and the disordered CG and CG' atoms of Iva(17). Refinement converged to *R*<sub>1</sub> = 0.0795 [on *F*, for 4700 reflections with *F*<sub>o</sub> ≥ 4( $\sigma$ )*F*<sub>o</sub>] and *wR*<sub>2</sub> = 0.276 (on *F*<sup>2</sup>) for all data. Other relevant crystal data are given in Table 2.

**Nuclear Magnetic Resonance and Molecular Dynamics Simulations.** A 15.3-mg sample of the *m*BrBz-protected heptapeptide methylamide were dissolved in 0.5 mL of CDCl<sub>3</sub> (*c* = 30 mmol/L). This solution was saturated with argon and residual oxygen was removed in an ultrasonic bath. The NMR measurements were

(20) Sheldrick, G. M. *SHELXS 86. Program for the Solution of Crystal Structures*; University of Göttingen, Germany, 1986.

(21) Sheldrick, G. M., *SHELXL 93. Program for Crystal Structure Refinement*; University of Göttingen, Germany, 1993.

**Table 3.** Relevant Backbone and Side Chain Torsion Angles (deg) for Molecules **A** and **B** (X-ray Structure) and Those Averaged over 100 ps RMD Trajectory<sup>a</sup> for the Terminally Blocked Heptapeptide

angle	molecule <b>A</b>	molecule <b>B</b>	averaged
		backbone	
$\phi_1$	-61.5(10)	-55.4(15)	-48(7)
$\psi_1$	-29.9(10)	-32.1(13)	-36(7)
$\omega_1$	-171.4(7)	-170.8(10)	
$\phi_2$	-52.8(9)	-57.0(15)	-46(7)
$\psi_2$	-32.3(8)	-29.6(13)	-46(7)
$\omega_2$	-175.3(6)	-179.5(9)	
$\phi_3$	-51.0(9)	-48.4(14)	-64(7)
$\psi_3$	-41.6(9)	-33.1(12)	-22(7)
$\omega_3$	-171.2(7)	-170.9(8)	
$\phi_4$	-54.7(9)	-54.0(10)	-43(7)
$\psi_4$	-32.7(9)	-26.3(9)	-29(7)
$\omega_4$	-175.0(7)	-176.8(6)	
$\phi_5$	-53.1(9)	-51.2(8)	-43(7)
$\psi_5$	-32.9(9)	-37.9(8)	-42(6)
$\omega_5$	-178.1(7)	-178.2(6)	
$\phi_6$	-51.6(9)	-51.2(9)	-55(7)
$\psi_6$	-45.1(9)	-41.6(9)	-51(6)
$\omega_6$	-175.5(8)	-176.5(7)	
$\phi_7$	-78.0(12)	-56.2(10)	-51(6)
$\psi_7$	-8.0(15)	-42.8(10)	-42(8)
$\omega_7$	-178.1(12)	-176.6(9)	
		side chains	
$\chi_{11}$	-74.0(10)	176.6(21)	66(8)
$\chi_{21,1}$	60.9(9)	168.1(16)	58(6)
$\chi_{21,2}$	-171.9(8)	-75.2(28); 42.1(19)	
$\chi_{31}$	170.9(9)	165.6(13)	-174(6)
$\chi_{41,1}$	169.2(9)	64.7(9)	169(6)
$\chi_{41,2}$	-64.0(9)	-171.2(9)	
$\chi_{51}$	-178.8(8)	176.8(6)	-170(5)
$\chi_{52,1}$	92.3(8)	89.9(7)	97(9)
$\chi_{52,2}$	-88.0(9)	-88.0(7)	
$\chi_{61,1}$	166.6(8)	171.4(9)	167(5)
$\chi_{61,2}$	-70.6(9)	-61.5(9)	
$\chi_{71}$	-61.6(10)	-178.9(15); -78.8(21)	-165(8)

<sup>a</sup> Reference 42.**Table 4.** Intra- and Intermolecular H-Bond Parameters for the Terminally Blocked Heptapeptide (X-ray Structure)

donor	acceptor	symmetry	distance (Å)		angle (deg)
D-H	A	operations of A	D...A	H...A	D-H...A
intramolecular					
N3	O0A	x, y, z	3.335(10)	2.497(9)	164.8(2)
N4	O1	x, y, z	3.034(8)	2.233(8)	154.9(2)
N5	O2	x, y, z	3.068(8)	2.284(8)	151.6(2)
N6	O3	x, y, z	3.185(8)	2.371(8)	158.1(2)
N7	O4	x, y, z	2.962(9)	2.264(9)	138.3(2)
N8	O5	x, y, z	2.864(13)	2.074(14)	152.4(4)
N13	O0B	x, y, z	3.246(11)	2.427(11)	159.3(3)
N14	O11	x, y, z	3.004(9)	2.151(8)	171.2(2)
N15	O12	x, y, z	3.136(10)	2.280(10)	173.6(3)
N16	O13	x, y, z	3.132(8)	2.318(8)	157.9(2)
N17	O14	x, y, z	2.995(8)	2.273(8)	141.6(2)
N18	O15	x, y, z	2.985(9)	2.358(9)	130.1(2)
intermolecular					
N1	O16	1 + x, y, 1 + z	2.892(8)	2.040(8)	170.8(2)
N2	O17	1 + x, y, 1 + z	3.232(9)	2.614(9)	129.6(2)
N11	O7	x, y, z	2.949(11)	2.329(13)	129.3(3)

performed on a Bruker AMX 600 instrument ( $B_0 = 14.1$  T). 1D experiments were performed in the range 300–260 K to find the optimal measuring conditions. An optimum between signal dispersion and line broadening was found at 270 K, and the 2D experiments were performed at this temperature. The  $^1\text{H}$  spectra were recorded with 128 scans, a sweep width of 5319.15 Hz, and a digital resolution of 16384 data points. The acquisition time was 1.54 s and the relaxation delay 1.0 s. For the  $^{13}\text{C}$  spectra 8196 scans were recorded at the sweep width

**Table 5.** Assignment of  $^1\text{H}$  and  $^{13}\text{C}$  NMR Resonances for the Terminally Blocked Heptapeptide<sup>a</sup>

residue	$^1\text{H}$	$\delta$	$^{13}\text{C}$	$\delta$	residue	$^1\text{H}$	$\delta$	$^{13}\text{C}$	$\delta$
mBrBz			C1	135.6	( $\alpha\text{Me}$ )Phe <sup>5</sup> NH	7.97	CO	173.7	
	H2	8.08	C2	130.9			C $\alpha$	60.2	
			C3	122.3	H $\beta$ Me	1.41	C $\beta$ Me	20.2	
	H4	7.52	C4	134.6	H $\beta^R$	3.03	C $\beta$	46.0	
	H5	7.18	C5	130.8	H $\beta^S$	3.33			
	H6	7.96	C6	126.2			C1	135.5	
Iva <sup>1</sup>			CO	166.4	H2,6	7.23	C2,6	130.6	
	NH	8.36	CO	172.9	H3	7.23	C3	127.8	
			C $\alpha$	61.2	H4	7.25	C4	126.5	
	H $\beta$ Me	1.55	C $\beta$ Me	20.3	H5	7.26	C5	127.8	
	H $\beta'$	2.02	C $\beta$	32.1	( $\alpha\text{Me}$ )Val <sup>6</sup> NH	7.63	CO	174.1	
	H $\beta''$	1.95					C $\alpha$	63.2	
	H $\gamma$ Me	0.97	C $\gamma$	8.2	H $\beta$ Me	1.32	C $\beta$ Me	14.8	
	( $\alpha\text{Me}$ )Val <sup>2</sup> NH	6.78	CO	171.8	H $\beta$	2.19	C $\beta$	35.3	
			C $\alpha$	62.0	H $\gamma^R$	1.14	C $\gamma'$	18.4	
			H $\beta$ Me	1.51	C $\beta$ Me	20.2	H $\gamma^S$	0.89	C $\gamma''$
(Iva) <sup>3</sup>	H $\beta$	1.91	C $\beta$	35.6	Iva <sup>7</sup> NH	7.45	CO	176.1	
	H $\gamma'$	0.85	C $\gamma'$	17.2			C $\alpha$	60.1	
	H $\gamma''$	0.83	C $\gamma''$	17.5	H $\beta$ Me	1.47	C $\beta$ Me	19.1	
	NH	7.83	CO	174.2	H $\beta^S$	1.94	C $\beta$	32.5	
			C $\alpha$	60.4	H $\beta^R$	1.83			
			H $\beta$ Me	1.53	C $\beta$ Me	20.8	H $\gamma$ Me	0.92	C $\gamma$
(Iva) <sup>4</sup>	H $\beta'$	1.96	C $\beta$	32.9	NHMe	NH	7.37		
	H $\beta''$	1.96				HMe	2.40	CMe	26.4
	H $\gamma$ Me	1.06	C $\gamma$	8.7					
	( $\alpha\text{Me}$ )Val <sup>4</sup> NH	7.71	CO	166.5					
			C $\alpha$	62.7					
			H $\beta$ Me	1.41	C $\beta$ Me	16.7			
		H $\beta$	2.12	C $\beta$	35.4				
		H $\gamma^S$	1.11	C $\gamma'$	17.9				
		H $\gamma^R$	0.98	C $\gamma''$	17.3				

<sup>a</sup> The spectra were recorded in  $\text{CDCl}_3$  ( $c = 30$  mmol/L) at 270 K. The prochirality is indicated by superscripts.

of 31250.0 Hz and a digital resolution of 65536 data points. The acquisition time was 1.05 s and the relaxation delay 4.0 s. The NOESY<sup>22</sup> spectrum was recorded with a sweep width of 5319.15 Hz in both dimensions and a digital resolution of 512 in  $F_1$  and 4096 in  $F_2$ . The mixing time was 100 ms, the acquisition time 385 ms, and the relaxation delay 1.3 s. For the data processing  $F_1$  was zero-filled to 1024 points. Subsequently, in  $F_1$  and  $F_2$  a squared sine bell function shifted by  $\pi/2$  was used for apodization. The DEPT-HMQC<sup>23</sup> spectrum was recorded with a swept width of 21739.13 Hz in  $F_1$  and 5319.15 Hz in  $F_2$ . The digital resolution was 512 data points in  $F_1$  and 4096 in  $F_2$ . A BIRD pulse was used to suppress the  $^1\text{H}$ - $^{13}\text{C}$  signals. For the data processing  $F_1$  was zero-filled to 1024 points. Subsequently, in  $F_1$  and  $F_2$  a squared sine bell function shifted by  $\pi/2$  was used for apodization. The HMBC<sup>24</sup> spectrum was recorded with a swept width of 21739.13 Hz in  $F_1$  and 5319.15 Hz in  $F_2$ . The digital resolution was 512 data points in  $F_1$  and 8192 in  $F_2$ . The relaxation delay was 1.3 s. For the data processing in  $F_1$  a linear prediction of 512 points using 8 coefficients was performed. Subsequently, in  $F_1$  and  $F_2$  a squared sine bell function shifted by  $\pi/2$  was used for apodization.

A set of interproton distances was determined from a quantitative evaluation of the NOESY spectrum. For calibration the cross-peak between the geminal ( $\alpha\text{Me}$ )Phe<sup>5</sup> H $\beta$  protons was used. An intensity correction for the cross-peaks of methyl groups (dividing the cross-peak volumes by three) was applied. The limits of the distance restraints were generated by adding/subtracting 10% of the NOE distance. In addition, a pseudoatom correction for methyl groups and the nondiastereotopically assigned protons has to be taken into account.

(22) Jeener, J.; Meier, B. H.; Bachmann, P.; Ernst, R. R. *J. Chem. Phys.* **1979**, *71*, 4546–4553.(23) Kessler, H.; Schmieder, P.; Kurz, M. *J. Magn. Reson.* **1989**, *85*, 400–405.(24) Bax, A.; Summers, M. F. *J. Am. Chem. Soc.* **1986**, *108*, 2093–2094.

**Table 6.** NOE Derived Distance Restraints, Calculated Distances in the Averaged Minimized MD Structure and in the X-ray Structure of Molecules **A** and **B** ( $\chi_2 = -75^\circ$ ,  $\chi_7 = -179^\circ$ ) for the Terminally Blocked Heptapeptide and in an Idealized  $\alpha$ -Helix<sup>a</sup>

atom 1	atom 2	lower limit	upper limit	$D_{MD}$	X-ray		$\alpha$ -helix
					mol A	mol B	
mBrBz H2	Iva <sup>1</sup> HN	3.00	3.67	<b>4.44</b>			<b>4.44</b>
mBrBz H6	Iva <sup>1</sup> HN	1.86	2.28	2.01			2.01
( $\alpha$ Me)Val <sup>2</sup> HN	Iva <sup>1</sup> HN	2.32	2.84	2.97	2.69	2.75	2.75
mBrBz H2	Iva <sup>3</sup> HN	3.55	4.34	3.39			3.64
mBrBz H2	mBrBz H4	3.97	4.86	4.27			4.27
mBrBz H6	mBrBz H5	1.94	2.37	2.44			2.44
Iva <sup>3</sup> HN	( $\alpha$ Me)Val <sup>2</sup> HN	2.29	2.80	2.82	2.80	2.70	2.52
( $\alpha$ Me)Val <sup>6</sup> HN	NHMe HN	3.01	3.68	3.95	<b>4.05</b>	<b>4.42</b>	<b>4.13</b>
mBrBz H4	mBrBz H5	2.08	2.54	2.48			2.48
( $\alpha$ Me)Phe <sup>5</sup> HN	( $\alpha$ Me)Phe <sup>5</sup> H $\beta^{proR}$	1.88	2.30	2.25	2.36	2.40	2.46
( $\alpha$ Me)Phe <sup>5</sup> HN	( $\alpha$ Me)Phe <sup>5</sup> H $\beta^{proS}$	1.95	2.38	2.43	2.48	2.44	2.40
( $\alpha$ Me)Val <sup>6</sup> HN	( $\alpha$ Me)Phe <sup>5</sup> H $\beta^{proR}$	2.82	3.45	<b>3.81</b>	<b>4.02</b>	<b>3.91</b>	<b>3.88</b>
( $\alpha$ Me)Val <sup>6</sup> HN	( $\alpha$ Me)Phe <sup>5</sup> H $\beta^{proS}$	2.28	2.79	2.61	2.75	2.55	2.74
Iva <sup>1</sup> HN	Iva <sup>1</sup> H $\beta$ Me	2.81	4.12	3.48	3.53	3.45	3.60
mBrBz H2	Iva <sup>3</sup> Hy	2.90	4.23	4.38			3.53
mBrBz H2	( $\alpha$ Me)Val <sup>2</sup> Hy	3.55	4.95	5.14			<b>6.79</b>
( $\alpha$ Me)Phe <sup>5</sup> HN	( $\alpha$ Me)Val <sup>4</sup> H $\beta$	2.29	2.80	2.95	2.80	<b>4.09</b>	2.93
Iva <sup>3</sup> HN	( $\alpha$ Me)Val <sup>4</sup> H $\beta$	3.37	4.12	<b>4.50</b>	<b>4.92</b>	<b>5.00</b>	<b>4.53</b>
Iva <sup>3</sup> HN	Iva <sup>3</sup> H $\beta$ Me	2.57	3.86	3.68	3.48	3.46	3.69
Iva <sup>3</sup> HN	( $\alpha$ Me)Val <sup>2</sup> Hy	2.23	5.39	3.59	3.50	4.27	3.62
( $\alpha$ Me)Val <sup>4</sup> HN	Val <sup>4</sup> H $\beta$	1.87	2.29	2.20	2.36	2.43	2.17
( $\alpha$ Me)Val <sup>4</sup> HN	Val <sup>4</sup> H $\gamma^{proR}$	2.60	3.89	<b>4.34</b>	<b>4.37</b>	<b>3.00</b>	<b>4.36</b>
( $\alpha$ Me)Val <sup>4</sup> HN	Val <sup>2</sup> Hy	3.77	7.59	5.74	5.57	5.78	5.96
( $\alpha$ Me)Val <sup>6</sup> HN	Val <sup>6</sup> H $\beta$	1.88	2.30	2.24	2.39	2.43	2.25
( $\alpha$ Me)Val <sup>6</sup> HN	Iva <sup>3</sup> H $\beta$ Me	2.97	4.30	4.04	4.13	4.10	4.51
( $\alpha$ Me)Val <sup>6</sup> HN	( $\alpha$ Me)Val <sup>6</sup> H $\beta$ Me	2.87	4.19	3.64	3.51	3.50	3.70
( $\alpha$ Me)Val <sup>6</sup> HN	Iva <sup>3</sup> Hy	3.61	5.01	5.04	<b>5.47</b>	<b>5.29</b>	<b>6.58</b>
( $\alpha$ Me)Val <sup>6</sup> HN	( $\alpha$ Me)Val <sup>6</sup> H $\gamma^{proR}$	2.87	4.19	4.44	4.36	4.41	4.45
( $\alpha$ Me)Val <sup>6</sup> HN	( $\alpha$ Me)Val <sup>6</sup> H $\gamma^{proS}$	2.28	3.53	3.26	2.87	2.78	3.39
Iva <sup>7</sup> HN	( $\alpha$ Me)Val <sup>6</sup> H $\beta$	2.29	2.80	2.53	2.40	2.65	2.87
Iva <sup>7</sup> HN	Iva <sup>7</sup> H $\beta$ Me	2.70	4.00	3.62	3.58	3.48	3.66
Iva <sup>7</sup> HN	( $\alpha$ Me)Val <sup>6</sup> H $\beta$ Me	3.72	5.13	4.47	4.33	4.37	4.41
Iva <sup>7</sup> HN	( $\alpha$ Me)Val <sup>6</sup> H $\gamma^{proS}$	3.51	4.91	4.79	4.56	4.62	5.00
Iva <sup>7</sup> HN	( $\alpha$ Me)Val <sup>4</sup> H $\gamma^{proR}$	3.79	5.21	<b>5.59</b>	5.17	<b>6.09</b>	<b>6.30</b>
Iva <sup>7</sup> HN	Iva <sup>7</sup> Hy	2.47	3.75	<b>4.29</b>	2.95	<b>4.32</b>	<b>4.31</b>
NHMe HN	NHMe HMe	2.27	3.52	2.61	2.46	2.50	2.61
NHMe HN	Iva <sup>7</sup> H $\beta^{proR}$	2.46	3.01	<b>3.61</b>	3.20	<b>3.71</b>	<b>3.62</b>
NHMe HN	Iva <sup>7</sup> H $\beta^{proS}$	2.53	3.10	2.42	<b>4.13</b>	2.32	2.45
NHMe HN	Iva <sup>7</sup> H $\beta$ Me	3.31	4.68	4.40	4.12	4.32	4.39
NHMe HN	( $\alpha$ Me)Val <sup>6</sup> H $\beta$ Me	3.92	5.35	5.18	4.47	4.80	5.17
NHMe HN	( $\alpha$ Me)Val <sup>4</sup> H $\gamma^{proR}$	4.07	5.52	5.34	5.46	<b>6.48</b>	<b>6.20</b>
NHMe HN	Iva <sup>7</sup> Hy	3.49	4.87	4.47	4.93	4.26	4.50
( $\alpha$ Me)Val <sup>2</sup> HN	Iva <sup>1</sup> Hy	3.26	4.62	3.21	4.86	4.44	3.09
( $\alpha$ Me)Val <sup>2</sup> HN	( $\alpha$ Me)Val <sup>2</sup> Hy	1.93	4.95	3.42	3.36	3.28	3.43
( $\alpha$ Me)Phe <sup>5</sup> H $\beta^{proR}$	( $\alpha$ Me)Val <sup>6</sup> H $\beta$ Me	4.25	5.72	<b>6.05</b>	5.96	5.90	5.99
( $\alpha$ Me)Phe <sup>5</sup> H $\beta^{proS}$	( $\alpha$ Me)Val <sup>6</sup> H $\beta$ Me	3.18	4.54	4.58	4.50	4.49	4.55
( $\alpha$ Me)Phe <sup>5</sup> H $\beta^{proR}$	( $\alpha$ Me)Val <sup>2</sup> Hy	3.09	6.62	6.08	5.67	5.84	<b>7.30</b>
( $\alpha$ Me)Phe <sup>5</sup> H $\beta^{proS}$	( $\alpha$ Me)Val <sup>2</sup> Hy	2.83	6.25	6.24	5.38	6.33	<b>6.58</b>
( $\alpha$ Me)Phe <sup>5</sup> H $\beta^{proS}$	( $\alpha$ Me)Val <sup>6</sup> H $\gamma^{proS}$	3.58	4.98	4.33	4.61	4.35	4.18
NHMe HMe	( $\alpha$ Me)Val <sup>6</sup> H $\beta$ Me	4.56	7.07	6.70	6.45	6.06	6.74
( $\alpha$ Me)Val <sup>6</sup> H $\beta$	Iva <sup>3</sup> H $\beta$ Me	3.01	4.35	4.70	4.80	5.02	3.42
( $\alpha$ Me)Val <sup>6</sup> H $\beta$	Iva <sup>7</sup> H $\beta$ Me	3.55	4.95	5.02	4.71	4.65	4.83
( $\alpha$ Me)Val <sup>6</sup> H $\beta$	( $\alpha$ Me)Val <sup>6</sup> H $\beta$ Me	3.04	4.38	3.86	3.86	3.85	3.86
( $\alpha$ Me)Val <sup>6</sup> H $\beta$	( $\alpha$ Me)Val <sup>6</sup> H $\gamma^{proR}$	2.18	3.42	2.50	2.44	2.48	2.50
( $\alpha$ Me)Val <sup>4</sup> H $\beta$	Iva <sup>1</sup> H $\beta$ Me	3.25	4.61	4.72	4.51	4.08	3.33
( $\alpha$ Me)Val <sup>4</sup> H $\gamma^{proR}$	Iva <sup>3</sup> H $\beta$	3.03	7.52	7.78	7.22	6.39	7.36
Iva <sup>7</sup> H $\beta^{proS}$	Iva <sup>7</sup> H $\beta$ Me	2.66	3.95	3.89	2.98	3.76	3.89
Iva <sup>7</sup> H $\beta^{proS}$	Iva <sup>7</sup> Hy	2.50	3.78	2.48	2.41	2.38	2.48
( $\alpha$ Me)Val <sup>6</sup> H $\gamma^{proR}$	( $\alpha$ Me)Val <sup>6</sup> H $\beta$ Me	2.74	5.04	3.88	3.63	3.60	3.88
( $\alpha$ Me)Val <sup>6</sup> H $\gamma^{proS}$	( $\alpha$ Me)Val <sup>6</sup> H $\beta$ Me	2.52	4.80	3.46	3.41	3.47	3.46
Iva <sup>3</sup> Hy	( $\alpha$ Me)Val <sup>6</sup> H $\beta$ Me	4.05	6.51	<b>7.09</b>	<b>8.35</b>	<b>8.06</b>	<b>9.70</b>
( $\alpha$ Me)Phe <sup>5</sup> HN	( $\alpha$ Me)Val <sup>4</sup> HN	2.18	2.67	2.81	2.77	2.79	2.58
( $\alpha$ Me)Phe <sup>5</sup> HN	( $\alpha$ Me)Val <sup>6</sup> HN	2.13	2.60	2.73	2.88	2.86	2.44
Iva <sup>1</sup> HN	Iva <sup>1</sup> Hy	3.01	4.34	3.15	3.15	4.39	3.05
( $\alpha$ Me)Phe <sup>5</sup> HN	( $\alpha$ Me)Val <sup>6</sup> H $\beta$	3.45	4.22	<b>4.61</b>	<b>4.96</b>	<b>4.93</b>	4.32
( $\alpha$ Me)Val <sup>4</sup> HN	( $\alpha$ Me)Val <sup>4</sup> H $\beta$ Me	2.78	4.09	3.54	3.47	3.47	3.68
( $\alpha$ Me)Val <sup>6</sup> HN	Iva <sup>7</sup> H $\beta^{proR}$	3.26	3.99	<b>4.49</b>	<b>4.78</b>	<b>5.07</b>	4.18
Iva <sup>7</sup> HN	Iva <sup>7</sup> H $\beta^{proR}$	1.96	2.39	2.15	2.33	2.36	2.21
Iva <sup>7</sup> HN	Iva <sup>7</sup> H $\beta^{proS}$	2.13	2.60	2.40	3.53	2.48	2.39
( $\alpha$ Me)Val <sup>2</sup> HN	( $\alpha$ Me)Val <sup>2</sup> H $\beta$ Me	2.55	3.83	3.58	3.46	3.53	3.68
( $\alpha$ Me)Phe <sup>5</sup> H $\beta^{proS}$	( $\alpha$ Me)Phe <sup>5</sup> H $\beta$ Me	2.90	4.22	3.90	3.82	3.80	3.90
( $\alpha$ Me)Phe <sup>5</sup> H $\beta^{proR}$	( $\alpha$ Me)Phe <sup>5</sup> H $\beta$ Me	2.53	3.82	3.16	2.99	2.95	3.16
NHMe HMe	Iva <sup>7</sup> H $\beta$ Me	4.69	7.21	5.82	5.43	5.54	5.82
NHMe HMe	( $\alpha$ Me)Phe <sup>5</sup> H $\beta$ Me	2.90	5.22	4.57	3.96	4.95	5.45
( $\alpha$ Me)Val <sup>6</sup> H $\beta$	( $\alpha$ Me)Val <sup>4</sup> H $\beta$ Me	3.53	4.92	4.10	4.31	4.20	<b>5.74</b>
( $\alpha$ Me)Val <sup>4</sup> H $\beta$	( $\alpha$ Me)Val <sup>2</sup> H $\beta$ Me	3.82	5.24	4.73	4.68	5.33	<b>5.78</b>

<sup>a</sup> Significant violations are indicated in bold.

**Table 7.** H-Bond Population during the Last 100 ps of the RMD (>1%) for the Terminally Blocked Heptapeptide

acceptor	donor	pattern ( $i \leftarrow x$ )	population (%)
<i>m</i> BrBz O=C	Iva <sup>3</sup> NH	$i + 3$	99
Iva <sup>1</sup> O=C	( $\alpha$ Me)Val <sup>4</sup> NH	$i + 3$	7
( $\alpha$ Me)Val <sup>2</sup> O=C	( $\alpha$ Me)Phe <sup>5</sup> NH	$i + 3$	51
Iva <sup>3</sup> O=C	( $\alpha$ Me)Val <sup>6</sup> NH	$i + 3$	100
( $\alpha$ Me)Val <sup>4</sup> O=C	Iva <sup>7</sup> NH	$i + 3$	39
( $\alpha$ Me)Val <sup>4</sup> O=C	NHMe	$i + 4$	53
( $\alpha$ Me)Phe <sup>5</sup> O=C	NHMe	$i + 3$	11

Thus, upper limits of NOE + 0.9 Å for methylene groups, NOE + 1.0 Å for methyl groups, and NOE + 2.1 Å for the *isopropyl* group (Val) were used.

Simulated annealing (SA) and molecular dynamics (MD) calculations were performed with the MSI Discover program using the CVFF force field.<sup>25</sup> The SA started with a manually built, extended conformation of the backbone. With this structure high-temperature dynamics at 1000 K (random velocity initialization according to the Boltzmann distribution) with downscaled force-field terms was performed. During the following downscaling of the temperature to 100 K the force-field terms were increased to their normal values. Each SA cycle was finished by a short minimization. The ten structures with the lowest total energy (including NOE distance restraints) were checked for convergence (mean backbone RMSD = 0.23 Å) and NOE distance violation (no distance restraint violation  $\geq 0.3$  Å). The structure with the lowest NOE distance violation was chosen for further rMD refinement in explicit chloroform. For that purpose the resulting SA structure was surrounded by a cubic box of chloroform (length: 32 Å, 176 CHCl<sub>3</sub> molecules). This system was minimized and heated to 270 K within six steps. Subsequently, the NOE distance restraints were reduced from 50 kcal/mol Å<sup>2</sup> to 5 kcal/mol Å<sup>2</sup> in four steps of 20 ps. After an additional 40-ps equilibration, data were recorded and analyzed for 100 ps.

## Results and Discussion

**Crystal-State Conformational Analysis.** We determined by X-ray diffraction the molecular and crystal structure of the terminally blocked heptapeptide Z-[L-Iva-L-( $\alpha$ Me)Val]<sub>2</sub>-L-( $\alpha$ Me)Phe-L-( $\alpha$ Me)Val-L-Iva-NHMe. A view perpendicular to the helix axis of the two independent molecules (**A** and **B**) in the asymmetric unit is illustrated in Figure 1. Relevant backbone and side-chain torsion angles<sup>26</sup> are given in Table 3. In Table 4 the intra- and intermolecular H-bond parameters are listed.

Both molecules **A** and **B** are right-handed 3<sub>10</sub>-helices,<sup>4</sup> stabilized by six consecutive intramolecular H bonds between the C=O group of residue  $i$  and the N-H group of residue  $i + 3$ . The right-handed helical screw sense is dictated by the known conformational bias of L-Iva (with a linear side chain)<sup>13,14</sup> and L-( $\alpha$ Me)Val (with a  $\beta$ -branched side chain).<sup>13,15</sup> The values of the  $\phi, \psi$  backbone torsion angles, as averaged for the first six residues of molecule **A** and all seven residues of molecule **B**, are  $-53.7^\circ$ ,  $-35.2^\circ$ , close to those typical for peptide 3<sub>10</sub>-helices ( $-57^\circ$ ,  $-30^\circ$ ).<sup>4</sup> The only significant deviation from such values is found at the C-terminal Iva<sup>7</sup> residue of molecule **A**, which adopts  $\phi, \psi$  values characteristic of the  $i + 2$  position of a type-I  $\beta$ -bend.<sup>27-29</sup> Therefore, while molecule **B** is a regular 3<sub>10</sub>-helix all the way through the main chain, formed by a succession of six type-III  $\beta$ -bends,<sup>27-29</sup> in molecule

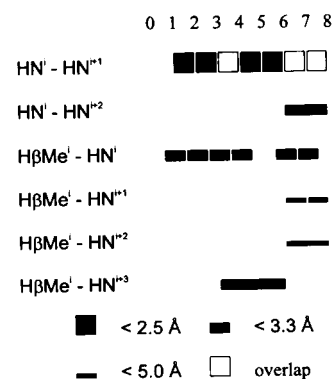


**Figure 2.** Summary of the NOE-derived backbone distances. The width of the bars indicates the NOE intensity. A white square shows a NOE that was not used during calculations due to overlap. The numbers are equivalent to the residue number with the exception of the N- and C-terminal protecting groups (0 = *m*BrBz, 8 = NHMe).

**A** the regularity of the helix is slightly distorted at the C-terminus, in that it is formed by five type-III  $\beta$ -bends followed by a nonhelical type-I  $\beta$ -bend. In both molecules, the N-terminal C=O...H-N intramolecular H bond is rather weak.<sup>30-32</sup>

Further conformational differences between molecules **A** and **B** are observed in the side-chain disposition of four corresponding residues.<sup>33</sup> Only the side-chain torsion angles of Iva<sup>3</sup> (*trans*), ( $\alpha$ Me)Phe<sup>5</sup> (*trans, skew<sup>+</sup>/skew<sup>-</sup>*), and ( $\alpha$ Me)Val<sup>6</sup> (*trans/gauche<sup>-</sup>*) in molecule **A** are closely matched by the corresponding torsion angles of Iva,<sup>13</sup> ( $\alpha$ Me)Phe,<sup>15</sup> and ( $\alpha$ Me)Val<sup>16</sup> residues in molecule **B**.

All of the peptide and (C-terminal) amide bonds are *trans* planar, although some distortion,  $|\Delta\omega > 8^\circ|$ , is seen for the  $\omega_1$  and  $\omega_3$  angles. The conformation of the urethane benzyloxy-carbonylamino group can be described by the torsion angles about the N1 (or N11)-C08, C08-OU, OU-C07, and C07-C01 bonds ( $\omega_0$ ,  $\theta^1$ ,  $\theta^2$ , and  $\theta^3$ , respectively).<sup>34</sup> While  $\omega_0$  and  $\theta^1$  are both *trans* [ $\omega_0 = -166.7(7)^\circ$  in **A** and  $176.1(11)^\circ$  in **B**;  $\theta^1 = 176.4(10)^\circ$  in **A** and  $-177.0(11)^\circ$  in **B**] and  $\theta^3$  has similar values [ $74.6(14)^\circ$  in **A** and  $84.1(11)^\circ$  in **B**], the values of  $\theta^2$  largely differ, being  $103.5(14)^\circ$  in **A** and  $-97.9(13)^\circ$  in **B**.

The two independent molecules are aligned head-to-tail in the crystal, with the helix axis along the [101] direction. The N-H group of the N-terminal Iva<sup>11</sup> of molecule **B** forms an intermolecular H bond with the C-terminal C=O group of Iva<sup>7</sup> of molecule **A** within the same asymmetric unit. Conversely, two intermolecular H bonds connect the N-terminus of molecule **A** to the C-terminus of a (1 + x, y, 1 + z) translated molecule **B**. Such H bonds involve the N-H groups of Iva<sup>1</sup> and ( $\alpha$ Me)Val<sup>2</sup> as the donors and the C=O groups of ( $\alpha$ Me)Val<sup>16</sup> and Iva,<sup>17</sup> respectively, of the symmetry equivalent molecule **B** as the acceptors. The latter H bond is very weak. Among the potential H bond donors only the N-H group of ( $\alpha$ Me)Val<sup>12</sup> does not participate in any H bond.

**NMR Spectroscopy and Molecular Dynamics Simulations.** Due to the high hydrophobicity of the terminally blocked heptapeptide side chains the NMR measurements were performed in CDCl<sub>3</sub> solution. During the analysis of the NMR

(25) Dauber-Osguthorpe, P.; Roberts, V. A.; Osguthorpe, D. J.; Wolff, J.; Genest, M.; Hagler, A. T. *Proteins: Struct. Funct. Genetics* **1988**, *4*, 31-47.

(26) IUPAC-IUB Commission on Biochemical Nomenclature. *Biochemistry* **1970**, *9*, 3471-3479.

(27) Venkatachalam, C. M. *Biopolymers* **1968**, *6*, 1425-1436.

(28) Toniolo, C. *CRC Crit. Rev. Biochem.* **1980**, *9*, 1-44.

(29) Rose, G. D.; Gierasch, L. M.; Smith, J. A. *Adv. Protein Chem.* **1985**, *37*, 1-109.

(30) Ramakrishnan, C.; Prasad, N. *Int. J. Protein Res.* **1971**, *3*, 209-231.

(31) Taylor, R.; Kennard, O.; Versichel, W. *Acta Crystallogr.* **1984**, *B40*, 280-288.

(32) Görbitz, C. H. *Acta Crystallogr.* **1989**, *B45*, 390-395.

(33) Benedetti, E.; Morelli, G.; Némethy, G.; Scheraga, H. A. *Int. J. Pept. Protein Res.* **1983**, *22*, 1-15.

(34) Benedetti, E.; Pedone, C.; Toniolo, C.; Dudek, M.; Némethy, G.; Scheraga, H. A. *Int. J. Pept. Protein Res.* **1983**, *21*, 163-181.

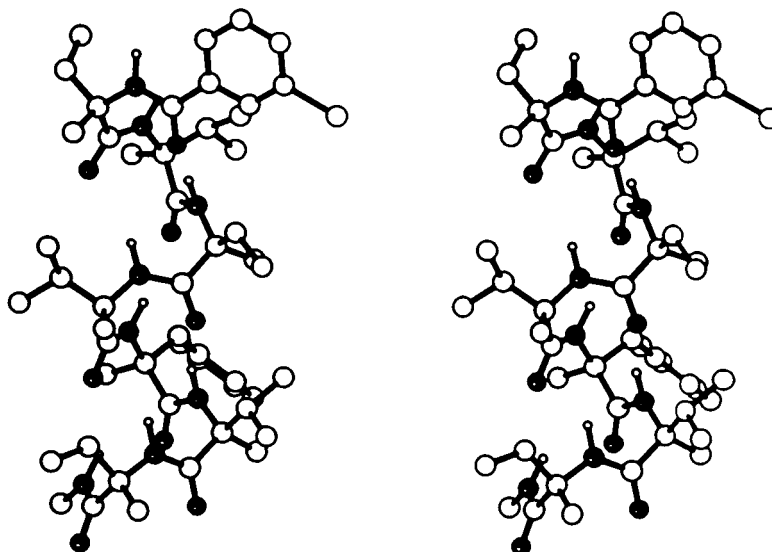


**Figure 3.** Stereoplot of the average, minimized rMD structure of *mBrBz*-[L-Iva-L-( $\alpha$ Me)Val]<sub>2</sub>-L-( $\alpha$ Me)Phe-L-( $\alpha$ Me)Val-L-Iva-NHMe.

experiments, signal assignment turned out to be the crucial problem. Mainly because of the low signal dispersion, it was not possible to assign unambiguously several NOESY cross-peaks. For the numerous methyl groups pseudoatom corrections on the NMR derived distances had to be taken into account. Because of the resulting limitations on the quality of the NMR derived constraints a simulated annealing strategy, instead of distance geometry, was used to search the conformational space. The refinement was performed with use of restrained MD in explicit chloroform.

For the chemical shift assignment of all proton and carbon resonances (Table 5) a combination of HMBC, HMQC, NOESY, and TOCSY<sup>35,36</sup> spectra was used. The assumption of a helical structure, which was initially required for assignment of the H<sup>N</sup> protons by using sequential H<sup>N</sup>-H<sup>N</sup> NOE's, could be later confirmed via the HMBC spectrum. The diastereotopic assignment of ( $\alpha$ Me)Phe<sup>5</sup> H <sup>$\beta$ R</sup>/H <sup>$\beta$ S</sup> and the Iva<sup>7</sup> H <sup>$\beta$ R</sup>/H <sup>$\beta$ S</sup> protons was performed on the basis of the different signal intensities of the H <sup>$\beta$</sup> -C' and H <sup>$\beta$</sup> -C <sup>$\beta$ Me</sup> cross-peaks in the HMBC experiments.<sup>37</sup> It was also possible to assign the diastereotopic  $\gamma$ -methyl groups of ( $\alpha$ Me)Val<sup>4</sup> and ( $\alpha$ Me)Val<sup>6</sup> by using NOE derived distances after the first converged simulated annealing calculation.

A set of interproton distances was determined from a quantitative evaluation of the NOESY spectrum. Altogether, 75 NOE derived distances, containing 35 intraresidual ( $i \rightarrow i$ ), 25 sequential ( $i \rightarrow i + 1$ ), and 15 long-range ( $i \rightarrow i + n$ ,  $n > 1$ ) constraints, were used (Table 6 and Figure 2).

The helical backbone arrangement was already indicated by the low <sup>13</sup>C-chemical shift dispersion and the series of sequential H<sup>N</sup><sub>*i*</sub>-H<sup>N</sup><sub>*i+1*</sub> NOE's. The major objective was to discriminate between a  $3_{10}$ -helical structure, as in the crystal structure of the Z-protected analogue (see above), and a possible  $\alpha$ -helical arrangement. To obtain no biased results, an only slightly optimized linear conformation was chosen as the starting structure for the SA calculations. The ten SA structures with the lowest total energy (including distance restraints) converged (backbone RMSD = 0.23 Å) to a conformation, that, according

to the Kabsch-Sander algorithm (Molmol 2.2.0),<sup>38,39</sup> can be classified as a  $3_{10}$ -helix from Iva<sup>1</sup> to ( $\alpha$ Me)Val<sup>6</sup>. The SA structure with the lowest NOE distance violation was chosen for further refinement with rMD in explicit chloroform (Table 3). Because of the lower force constants ( $K_{\text{NOE(SA)}/10}$ ), the distance restraint violation is not so good as the SA results, but the disagreements are limited to the N- and C-terminal regions which might be slightly disturbed by aggregation (see below).

The peptide seems to be quite rigid. The backbone RMSD referenced to the SA structure is 0.30 Å with a standard deviation of only 0.06 Å over the last 100 ps. This rigidity can also be seen in the small standard deviations of the dihedral angles listed in Table 3.

The H-bonding pattern (Table 7) gives a good hint on the secondary structure exhibited by the heptapeptide. It shows a clear preference for  $i \rightarrow i + 3$  hydrogen bonds. Only at the C-terminus can a significant population of an  $i \rightarrow i + 4$  H bond be observed. This three-center H bond<sup>40</sup> with Iva<sup>7</sup> NH and the C-terminal NHMe group acting as donors and the ( $\alpha$ Me)Val<sup>4</sup> C=O group as the acceptor seems to produce a new type of C-capping motif. The averaged, minimized conformation of the last 100 ps is depicted in Figure 3. It shows a  $3_{10}$ -helical conformation from residue 1 to residue 6. The backbone RMSD to the two conformers observed in the crystal state for the Z-protected analogue is 0.39 and 0.64 Å, respectively. It must be kept in mind that, according to Scheraga and co-workers,<sup>41</sup> normal molecular mechanics force fields have a tendency to prefer an  $\alpha$ -helix over a  $3_{10}$ -helix for peptides containing C <sup>$\alpha$</sup> -tetrasubstituted  $\alpha$ -amino acids. To show the preference of the experimental data for a  $3_{10}$ -helix, a restrained minimization starting with an  $\alpha$ -helix (the backbone dihedrals of the averaged, minimized rMD structure were set to  $\varphi = -65$  and  $\psi = -40$ )<sup>42</sup> was performed. The resulting structure showed a backbone RMSD of 0.15 Å referenced to the averaged, minimized rMD,  $3_{10}$ -helical structure.

(38) Kabsch, W.; Sander, C. *Biopolymers* **1983**, *22*, 2577-2637.

(39) Konradi, R.; Billeter, M.; Wüthrich, K. *J. Mol. Graph.* **1996**, *14*, 51-55.

(40) Taylor, R.; Kennard, O.; Versichel, W. *J. Am. Chem. Soc.* **1984**, *106*, 244-248.

(41) Paterson, Y.; Rumsey, S. M.; Benedetti, E.; Némethy, G.; Scheraga, H. A. *J. Am. Chem. Soc.* **1981**, *103*, 2947-2955.

(42) Shenderovich, M. D.; Köver, K. E.; Wilke, S.; Collins, N.; Hruby, V. J. *J. Am. Chem. Soc.* **1997**, *119*, 5833-5846.

(35) Braunschweiler, L.; Ernst, R. R. *J. Magn. Reson.* **1983**, *53*, 521-528.

(36) Bax, A.; Davis, D. G. *J. Magn. Reson.* **1985**, *65*, 355-360.

(37) Hoffmann, M.; Gehrke, M.; Bermel, W.; Kessler, H. *Magn. Reson. Chem.* **1989**, *27*, 877-886.

**Table 8.** List of Unambiguously Assigned Intermolecular NOEs for the Terminally Blocked Heptapeptide

		NOE (Å)
Iva <sup>1</sup> HN	NHMe HMe	3.99
Iva <sup>1</sup> HN	(αMe)Val <sup>6</sup> HMe	3.51
(αMe)Val <sup>2</sup> HN	NHMe HMe	3.92
(αMe)Val <sup>2</sup> HN	Iva <sup>7</sup> HβMe	3.67
Iva <sup>1</sup> HβMe	NHMe HMe	5.08
<i>m</i> BrBz H2	NHMe HMe	4.93
<i>m</i> BrBz H5	NHMe HMe	3.68

The crystal structure of the Z-protected analogue shows a head-to-tail aggregation of the  $3_{10}$ -helices. In CDCl<sub>3</sub> at low temperature the dipolar nature of the helical structure can also lead to significant aggregation. Indeed, there is experimental evidence for such a phenomenon in solution. A few intermolecular NOEs (Table 8) suggest aggregation on the time scale of the NOESY mixing time (100 ms). These NOEs are mainly observed between atoms at either termini of the helix. Although a direct comparison of the intermolecular distances in the cell of the X-ray structure with the NMR-derived NOE distances is difficult due to the two different N-terminal blocking groups, it gives a clear hint on a similar head-to-tail aggregation in the crystal state and in solution.

### Conclusions

To distinguish a  $3_{10}$ - versus an  $\alpha$ -helix by NMR spectroscopy one relevant problem is the design of appropriate prototypical peptide standards fully developed in each of the two secondary structures. As a first step in this direction, we synthesized by solution methods and fully characterized the conformationally restricted, N-blocked heptapeptide methylamide *m*BrBz-[L-Iva-L-(αMe)Val]<sub>2</sub>-L-(αMe)Phe-L-(αMe)Val-L-Iva-NHMe.

We were able to grow a single crystal and solve the X-ray diffraction structure of its synthetic precursor, the *N*<sup>α</sup>-benzyl-oxycarbonylated analogue. This modest modification at the N-terminus is not expected to modify the peptide secondary structure in any significant way.<sup>12,13</sup> However, what was assumed to be a rather routine task, *i.e.* a noncentrosymmetric structure containing 69 light (non-H) atoms, turned out to be a challenging problem owing to the occurrence of two independent molecules in the asymmetric unit, thus leading to a 138-atom

structure. Both peptide molecules are folded in the crystal state into a fully developed, regular, right-handed  $3_{10}$ -helical conformation, although in molecule **A** the backbone  $\varphi, \psi$  torsion angles of the C-terminal residue are distorted from the ideal values,<sup>4</sup> albeit slightly (by  $\sim 25^\circ$ ).

The NMR spectroscopy-simulated annealing-restrained molecular dynamics strategy used in this study allowed us to classify the 3D-structure of the terminally blocked heptapeptide in CDCl<sub>3</sub> solution as a rigid  $3_{10}$ -helix all the way from residue 1 to residue 6. A mixed  $3_{10}/\alpha$ -helical conformation appears to be populated at the C-terminus. Distinguishing between  $\alpha$ - and  $3_{10}$ -helical peptides is in general a difficult task, as there is essentially only one NOE constraint that is different in both structures by more than the usual error in distance measurements [ $d_{\alpha N}(i, i+2)$ ]. In addition, this distance is in the range of 4 Å, which is at the upper limit for getting distances in small molecules. In our peptide model, which lacks all CH<sup>α</sup> protons, we used the sum of all available experimental data and could prove that only a  $3_{10}$ -helix is observed in solution.

Further NMR studies of appropriately designed analogues, incorporating single and double substitutions with host *protein* amino acids, of this standard  $3_{10}$ -helical guest peptide based exclusively on *C*<sup>α</sup>-methylated amino acids will show whether this helix is still stable or has been modified into an  $\alpha$ -helical structure, and in the latter case, whether it is possible to analyze a potential equilibrium between these two biologically important secondary peptide structures by NMR spectroscopy.

**Acknowledgment.** Part of this work was supported by the Deutsche Forschungsgemeinschaft and the Fonds der Chemischen Industrie.

**Supporting Information Available:** Tables of crystal data and structure refinement, atomic coordinates, isotropic and anisotropic displacement parameters, bond lengths and angles, hydrogen coordinates, torsion angles, relevant backbone and side chain torsion angles, and intra- and intermolecular H-bond parameters for **1** (25 pages, print/PDF). See any current masthead page for ordering information and Web access instructions.

JA9731478